

# Rational Design, Synthesis, and Spectroscopic and Photophysical Properties of a Visible-Light-Excitable, Ratiometric, Fluorescent Near-Neutral pH Indicator Based on BODIPY

Noël Boens,<sup>\*,[a]</sup> Wenwu Qin,<sup>[a, b]</sup> Mukulesh Baruah,<sup>[a]</sup> Wim M. De Borggraeve,<sup>[a]</sup> Aleksander Filarowski,<sup>[a, c]</sup> Nick Smisdom,<sup>[d]</sup> Marcel Ameloot,<sup>[d]</sup> Luis Crovetto,<sup>[e]</sup> Eva M. Talavera,<sup>[e]</sup> and Jose M. Alvarez-Pez<sup>\*,[e]</sup>

**Abstract:** A visible-light-excitable, ratiometric, brightly fluorescent pH indicator for measurements in the pH range 5–7 has been designed and synthesized by conjugatively linking the BODIPY fluorophore at the 3-position to the pH-sensitive ligand imidazole through an ethenyl bridge. The probe is available as cell membrane permeable methyl ester 8-(4-carbomethoxyphenyl)-4,4-difluoro-3-[2-(1*H*-imidazol-4-yl)ethenyl]-1,5,7-trimethyl-3*a*,4*a*-diaz-4-bora-*s*-indacene (**I**) and corresponding water-soluble sodium carboxylate, sodium 8-(4-carboxylatophenyl)-4,4-difluoro-3-[2-(1*H*-imidazol-4-yl)ethenyl]-1,5,7-trimethyl-3*a*,4*a*-diaz-4-bora-*s*-indacene (**II**). The fluorescence quantum yield  $\Phi_f$  of ester **I** is very high (0.8–1.0) in the organic solvents tested. The fluorescence lifetime (ca. 4 ns) of **I** in organic solvents with varying polarity/polarizability (from cyclohexane to acetonitrile) is independent of the solvent with a fluorescence rate constant  $k_f$  of  $2.4 \times 10^8 \text{ s}^{-1}$ . Probe **I** is readily

loaded in the cytosol of live cells, where its high fluorescence intensity remains nearly constant over an extended time period. Water-soluble indicator **II** exhibits two acid–base equilibria in aqueous solution, characterized by  $pK_a$  values of 6.0 and 12.6. The  $\Phi_f$  value of **II** in aqueous solution is high: 0.6 for the cationic and anionic forms of the imidazole ligand, and 0.8 for neutral imidazole. On protonation–deprotonation in the near-neutral pH range, UV/Vis absorption and fluorescence spectral shifts along with isosbestic and pseudo-isoemissive points are observed. This dual-excitation and dual-emission pH indicator emits intense green-yellow fluorescence at lower pH and intense orange fluorescence at higher pH. The influence of ionic strength and buffer concentration

on the absorbance and steady-state fluorescence of **II** has also been investigated. The apparent  $pK_a$  of the near-neutral acid–base equilibrium determined by spectrophotometric and fluorometric titration is nearly independent of the added buffer and salt concentration. In aqueous solution in the absence of buffer and in the pH range 5.20–7.45, dual exponential fluorescence decays are obtained with decay time  $\tau_1 = 4.3 \text{ ns}$  for the cationic and  $\tau_2 = 3.3 \text{ ns}$  for the neutral form of **II**. The excited-state proton exchange of **II** at near-neutral pH becomes reversible on addition of phosphate ( $\text{H}_2\text{PO}_4^-/\text{HPO}_4^{2-}$ ) buffer, and a pH-dependent change of the fluorescence decay times is induced. Global compartmental analysis of fluorescence decay traces collected as a function of pH and phosphate buffer concentration was used to recover values of the deactivation rate constants of the excited cationic ( $k_{01} = 2.4 \times 10^8 \text{ s}^{-1}$ ) and neutral ( $k_{02} = 3.0 \times 10^8 \text{ s}^{-1}$ ) forms of **II**.

**Keywords:** dyes/pigments • fluorescent probes • pH indicators • photo-physics • sensors

[a] Prof. N. Boens, Prof. W. Qin, Dr. M. Baruah, Prof. W. M. De Borggraeve, Prof. A. Filarowski  
Department of Chemistry  
Katholieke Universiteit Leuven  
Celestijnenlaan 200f - bus 02404, 3001 Leuven (Belgium)  
E-mail: Noel.Boens@chem.kuleuven.be

[b] Prof. W. Qin  
Key Laboratory of Nonferrous Metal Chemistry and Resources  
Utilization of Gansu Province and State Key Laboratory  
of Applied Organic Chemistry  
College of Chemistry and Chemical Engineering  
Lanzhou University, Lanzhou 730000 (P. R. China)

[c] Prof. A. Filarowski  
Faculty of Chemistry, University of Wrocław  
F. Joliot-Curie 14, 50-383 Wrocław (Poland)

[d] N. Smisdom, Prof. M. Ameloot  
BIOMED, Universiteit Hasselt and transnational University Limburg  
Agoralaan, Gebouw C, 3590 Diepenbeek (Belgium)

[e] Dr. L. Crovetto, Prof. E. M. Talavera, Prof. J. M. Alvarez-Pez  
Department of Physical Chemistry  
University of Granada, Cartuja Campus  
Granada 18071 (Spain)  
E-mail: jalvarez@ugr.es



Supporting information for this article is available on the WWW under <http://dx.doi.org/10.1002/chem.201002280>. It contains solvatochromism of absorption ( $\bar{\nu}_{\text{abs}}$ ) and emission ( $\bar{\nu}_{\text{em}}$ ) maxima of **I**; ratiometric fluorometric titrations of **II** for the estimation of  $K_a$ ; pH dependence of the excitation and emission spectra of **II** (pH 10.75–12.54); pH dependence of fluorescence quantum yields of **II**; loading of UBimi in live HEK 293 cells; photostability and retention of UBimi in live HEK 293 cells; theory; experimental details; global compartmental analysis results of time-resolved fluorescence of **II**; and  $^1\text{H}$  NMR spectrum of **I**.

## Introduction

The design, synthesis, and spectroscopic/photophysical characterization of novel fluorescent chemosensors continue to be vibrant research topics.<sup>[1]</sup> Measurement of pH by fluorescence-based techniques is well established for both imaging and sensing applications.<sup>[2,3]</sup> Fluorescent near-neutral pH indicators that can quantify minor pH changes are especially attractive targets in molecular design and synthesis.

Because of their excellent characteristics, 4,4-difluoro-4-bora-3a,4a-diaza-*s*-indacene<sup>[4,5]</sup> (better known as BODIPY,<sup>[2]</sup> difluoroboron dipyrromethene) derivatives are favored fluorophores in the design of fluorescent probes. Indeed, the valuable qualities of BODIPY<sup>[4,5]</sup> comprise relatively high molar absorption coefficients and fluorescence quantum yields, narrow emission bandwidths with high peak intensities, robustness towards light and chemicals, and excitation/emission wavelengths in the visible spectral range (above 500 nm). Moreover, the spectroscopic properties of BODIPY derivatives can be fine-tuned by synthetically introducing suitable substituents at the right positions of the difluoroboron dipyrromethene core.

Difluoroboradiaza-*s*-indacenes with hydroxyaryl subunits have been reported as pH indicators in aqueous–organic mixed media.<sup>[6,7]</sup> These on/off pH indicators showed photo-induced electron transfer (PET) from the twisted and conjugatively uncoupled phenolate to the BODIPY subunit, causing fluorescence quenching at high pH. 8-(4'-Hydroxyphenyl)-substituted BODIPY derivatives<sup>[6]</sup> sense the alkaline pH range, while the tetrahydroxylated calix[4]arene derivative<sup>[7]</sup> is sensitive in the near-neutral pH range. An on/off 8-(4'-dimethylaminophenyl)-substituted BODIPY indicator has been reported for the acidic pH range.<sup>[8,9]</sup> Quenching by PET from the dimethylanilino group to the fluorophore accounts for quenching of emission in the uncharged form. Previously, we synthesized and spectroscopically characterized two water-soluble, on/off pH indicators with  $pK_a$  around 7.5 based on *o*-chlorophenol linked to the *meso* (8-) position<sup>[10]</sup> or through a vinyl bridge to the 3-position<sup>[11]</sup> of difluoroboron dipyrromethene. However, these indicators showed substantial amplification of fluorescence intensity at lower pH, without fluorescence spectral shift. A series of pH probes based on BODIPY with *meso*-anilino substituents have been described recently for imaging acidic endosomes in cancer cells.<sup>[12]</sup> These derivatives are almost non-fluorescent in basic media due to PET.

Here we describe the molecular design and synthesis of UBimi (*ultra-bright imidazole-based indicator*), that is, methyl ester **I** and its associated water-soluble sodium salt **II**, substituted with a 2-(1*H*-imidazol-4-yl)ethenyl group at the 3-position of the BODIPY core (Figure 1). We also investigate its solvent- and pH-dependent spectroscopic and photophysical properties. Furthermore, we explore the ground-state equilibrium between the protonated and neutral imidazole forms of **II** through spectrophotometric and fluorometric titrations. Next, the influence of the addition of salt and buffer on the apparent acidity constant of **II** mea-

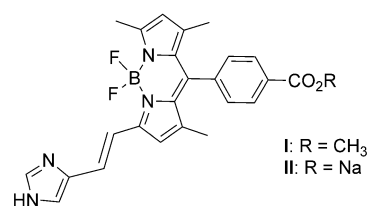


Figure 1. Chemical structure of UBimi: methyl ester **I** and carboxylate salt **II**.

sured by spectrophotometric and fluorometric titrations is investigated. Finally, the excited-state kinetics of **II** in aqueous solution is investigated by global compartmental analysis of the fluorescence decay surface, collected as a function of emission wavelength, pH, and buffer concentration. The major purpose of this work is to demonstrate that it is feasible, by judicious choice of fluorophore and ligand, to rationally design a near-neutral fluorescent pH probe which has many desirable properties. Note that intracellular pH measurements are beyond the scope of this paper.

## Results and Discussion

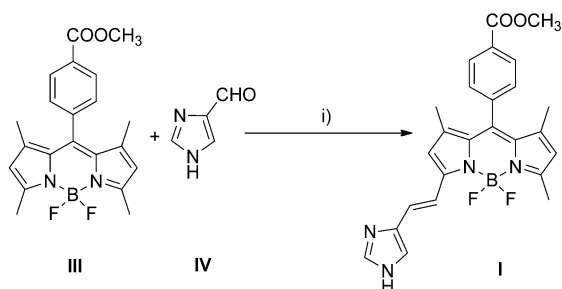
**Design of the fluorescent pH indicator:** Robustness of the indicator against chemicals and light, a ground-state  $pK_a$  value close to the actual pH one intends to measure, excitation and emission spectra in the visible wavelength range, intense fluorescence (requiring large molar absorption coefficients  $\epsilon(\lambda_{ex})$  at the excitation wavelength  $\lambda_{ex}$  and high fluorescence quantum yields  $\Phi_f$ , i.e., high dye brightness),<sup>[13]</sup> and spectral shifts of the excitation and/or emission spectrum on proton binding are all looked-for properties of the optimal fluorescent pH indicator.

We chose imidazole/imidazolium with its favorable  $pK_a$  of 7.0 to serve as pH-sensitive ligand for the near-neutral pH range. Substitution of imidazole generally leads to different  $pK_a$  values. Due to the electron-withdrawing character of BODIPY, it is expected that conjugatively linking the BODIPY fluorescent reporter subunit via an ethenyl bridge to imidazole will decrease the  $pK_a$  of imidazole in UBimi by approximately 1 unit compared to free imidazole. Imidazole itself exhibits two acid–base equilibria: between the cationic and neutral species with  $pK_a=7$  and between the neutral and anionic forms with  $pK_a=14$ .<sup>[14]</sup> We discuss this in detail below for pH indicator **II**.

Because of its many excellent properties, we selected BODIPY as key fluorophore for the novel pH indicator. Owing to its beneficial properties, many probe requirements are automatically fulfilled: (photo)chemical stability, bright fluorescence due to high  $\epsilon(\lambda_{ex})$  and  $\Phi_f$ , and excitation with visible light are all intrinsic to the BODIPY platform. The fluorescent probe UBimi entails conjugation of the imidazole pH-sensing subunit through an ethenyl linker to the BODIPY core at the 3-position. Based on the spectroscopic properties of BODIPY derivatives with ethenylphenyl sub-

stituents at the 3- (and 5-) position(s),<sup>[15]</sup> it is expected that conjugation of the imidazole ligand through an ethenyl linker at the 3-position will introduce a pronounced bathochromic shift of both absorption (excitation) and emission maxima compared to classic BODIPY fluorophores,<sup>[16]</sup> and will lead to elevated photostability,<sup>[17]</sup> high  $\Phi_f$  and  $\varepsilon(\lambda_{ex})$  values, and may produce spectral shifts on protonation–deprotonation. The pH-sensitive ligand is linked to the fluorophore by a condensation reaction of commercially available 1*H*-imidazole-4-carbaldehyde with a methyl group at the 3-position of BODIPY.<sup>[15]</sup> To increase the quantum yield  $\Phi_f$ , we chose a 4,4-difluoro-1,3,5,7-tetramethyl-4-bora-3*a*,4*a*-diazas-indacene analogue, because there is evidence that 1,3,5,7-tetramethyl-substituted boradiazaindacene has high  $\Phi_f$  values.<sup>[5,10,18]</sup> To ensure cell membrane permeability, a benzoate ester (in **I**), which can be converted to a water-soluble carboxylate salt (in **II**), either by saponification or by nonselective intracellular esterases, was introduced at the *meso* position (Figure 1). The  $\pi$  systems of BODIPY and an aromatic substituent at the *meso* position are highly twisted and hence electronically essentially decoupled (i.e., no conjugation is possible between the BODIPY core and its aromatic *meso* substituent).<sup>[8,19]</sup> Therefore, locating methyl benzoate at the *meso* position will minimally affect the spectral (UV/Vis absorption and emission) positions when it is converted to an ionic carboxylate group. Likewise, fluorescent pH indicators based on difluoroboron dipyrromethene in which a proton signaling subunit connected to the *meso* position is uncoupled from the fluorophore are never ratiometric.<sup>[6–10]</sup> An essential design principle for a ratiometric, fluorescent pH signaling system is to have conjugation between the pH- (i.e.,  $H^+$ -) sensitive subunit and the fluorophore.

**Synthesis of UBimi:** 8-(4-Carbomethoxyphenyl)-4,4-difluoro-3-[2-(1*H*-imidazol-4-yl)ethenyl]-1,5,7-trimethyl-3*a*,4*a*-diazas-indacene (**I**, Figure 1) was synthesized in 51% yield by condensation of 8-(4-carbomethoxyphenyl)-4,4-difluoro-1,3,5,7-tetramethyl-3*a*,4*a*-diazas-indacene (**III**) with 1*H*-imidazole-4-carbaldehyde (**IV**) with acetic acid/piperidine as catalyst (Scheme 1). Starting material **III** is a known compound and was prepared from methyl 4-formylbenzoate and 2,4-dimethylpyrrole by following a literature procedure.<sup>[11]</sup> The sodium carboxylate form of



Scheme 1. Synthesis of compound **I**. Conditions: i) toluene, piperidine, AcOH, molecular sieves, reflux, 30 min, 51%.

UBimi (**II**, Figure 1) was obtained by saponification with NaOH.

**Spectroscopic properties of I:** Solvatochromism of UBimi ester **I** was investigated in several solvents. Figure 2 shows

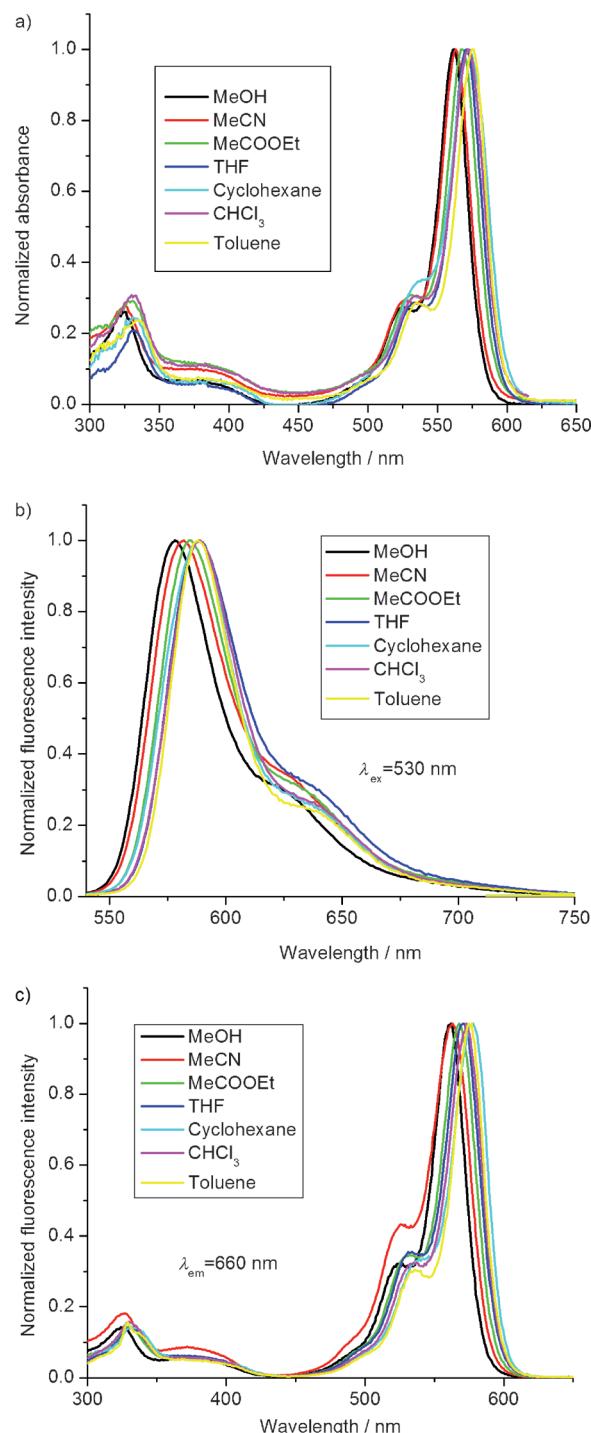


Figure 2. a) Absorption spectra of **I** in different solvents normalized to 1.0. b) Corresponding normalized fluorescence emission spectra (excitation at  $\lambda_{ex} = 530$  nm). c) Corresponding normalized excitation spectra (observed at  $\lambda_{em} = 660$  nm).

the normalized UV/Vis absorption and fluorescence excitation and emission spectra of **I** in various solvents. The absorption spectra are of similar shape to those of classic BODIPY dyes,<sup>[5,15,16,18]</sup> with an intense absorption band with a maximum  $\lambda_{\text{abs}}(\text{max})$  located between 562 nm (in methanol) and 575 nm (in toluene), assigned to the 0–0 band of the  $S_1 \leftarrow S_0$  transition, and a (more or less pronounced) shoulder on the high-energy side, attributed to the 0–1 vibrational band of the same transition. The  $\lambda_{\text{abs}}(\text{max})$  values are hardly affected by solvent polarity/polarizability, consistent with the absorption spectroscopic behavior of common BODIPY chromophores.<sup>[16,20]</sup> The solvent dependence of  $\bar{\nu}_{\text{abs}} [=1/\lambda_{\text{abs}}(\text{max})]$  is illustrated in Figure S1 (Supporting Information). In addition, a weaker, broad absorption band, attributed to the  $S_2 \leftarrow S_0$  transition, is found around 380 nm, the position of which is practically independent of solvent. Compared to classical BODIPY derivatives,  $\lambda_{\text{abs}}(\text{max})$  is redshifted by approximately 50–60 nm.<sup>[5,15,16,18,20]</sup> UBimi in cyclohexane, THF, and methanol is effectively optically transparent between 430 and 450 nm. The full width at half-height of the maximum of the main absorption band ( $\text{fwhm}_{\text{abs}}$ ) is narrow and nearly independent of solvent [ $(84 \pm 7) \times 10 \text{ cm}^{-1}$ ]. The molar absorption coefficients  $\epsilon_{\text{max}}$  at the absorption maximum  $\lambda_{\text{abs}}(\text{max})$  were determined in three solvents and are compiled in Table 1 together with other relevant spectroscopic and photophysical data.

In all solvents studied, compound **I** also exhibits typical BODIPY emission features (Figure 2), that is, a narrow, slightly Stokes-shifted band of mirror-image shape.<sup>[16]</sup> The maximum emission wavelength  $\lambda_{\text{em}}(\text{max})$  is in the 577–589 nm range. The near-independence of the Stokes shift  $\Delta\bar{\nu} [=1/\lambda_{\text{abs}}(\text{max}) - 1/\lambda_{\text{em}}(\text{max}) = (49 \pm 6) \times 10 \text{ cm}^{-1}]$  from the solvent indicates that there is no appreciable difference between the permanent dipole moments of ground and excited states.<sup>[21,22]</sup> The solvent dependence of  $\bar{\nu}_{\text{em}} [=1/\lambda_{\text{em}}(\text{max})]$  is shown in Figure S2 (Supporting Information). The fluorescence quantum yields  $\Phi_f$  for **I** are very high in all solvents studied ( $0.78 \leq \Phi_f \leq 1.00$ ). An important photophysical property of a fluorescent sensor is its brightness,<sup>[13]</sup> defined as the product of the fluorescence quantum yield  $\Phi_f$  and the molar absorption coefficient  $\epsilon(\lambda_{\text{ex}})$  at the excitation wavelength  $\lambda_{\text{ex}}$ . The brightness values of **I** calculated for the absorption

maximum (corresponding to  $\epsilon(\lambda_{\text{ex}}) = \epsilon_{\text{max}}$ ) in chloroform, ethyl acetate, and methanol were  $3.57 \times 10^4$ ,  $4.36 \times 10^4$ , and  $3.91 \times 10^4 \text{ L mol}^{-1} \text{ cm}^{-1}$ , respectively. To put these favorable values into perspective, we compare them with representative literature values for some fluorescein and rhodamine-based pH indicators useful at near-neutral pH. 2',7'-Bis(2-carboxyethyl)-5-(and -6-)carboxyfluorescein (BCECF) is currently the most popular fluorescent indicator for estimating intracellular, near-neutral pH.<sup>[23,24]</sup> The phenolic form of BCECF has  $\epsilon_{\text{max}} = 3.47 \times 10^4 \text{ L mol}^{-1} \text{ cm}^{-1}$  at 484 nm.<sup>[24]</sup> Since no  $\Phi_f$  data for BCECF in acidic solution are available, its brightness cannot be determined. The corresponding phenolate form has redshifted absorption spectra with increased molar absorption coefficients ( $\epsilon_{\text{max}} = 8.73 \times 10^4 \text{ L mol}^{-1} \text{ cm}^{-1}$  at 503 nm).<sup>[24]</sup> In combination with  $\Phi_f = 0.84$ ,<sup>[25]</sup> this yields a maximal brightness of  $7.33 \times 10^4 \text{ L mol}^{-1} \text{ cm}^{-1}$ . 2',7'-Bis(2-carboxypropyl)-5-(and -6-)carboxyfluorescein (BCPCF) is a homologue of BCECF.<sup>[25]</sup> As expected, it has similar  $pK_a$  values, absorption and emission maximum wavelengths, and  $\Phi_f$  values. Seminaphthorhodamine derivative 5-(and 6-)carboxy-SNARF-1 (C.SNARF-1)<sup>[2,26]</sup> is probably the second most widely used indicator for intracellular, near-neutral pH measurements. The phenolic form of C.SNARF-1 has  $\epsilon_{\text{max}} = 2.7 \times 10^4 \text{ L mol}^{-1} \text{ cm}^{-1}$  at 548 nm with  $\Phi_f = 0.03$ ,<sup>[2,3,26]</sup> yielding a brightness of only  $810 \text{ L mol}^{-1} \text{ cm}^{-1}$ . Its corresponding phenolate form has  $\epsilon_{\text{max}} = 4.8 \times 10^4 \text{ L mol}^{-1} \text{ cm}^{-1}$  at 576 nm with  $\Phi_f = 0.09$ ,<sup>[2,3,26]</sup> resulting in an increased, albeit low, brightness of  $4320 \text{ L mol}^{-1} \text{ cm}^{-1}$ . The phenolic form of 5-(and 6-)carboxy-SNAFL-1 (C.SNAFL-1, a seminaphthofluorescein derivative)<sup>[2,26]</sup> has  $\epsilon_{\text{max}} = 2.9 \times 10^4 \text{ L mol}^{-1} \text{ cm}^{-1}$  at 508 nm with  $\Phi_f = 0.32$ ,<sup>[2,3,26]</sup> resulting in a brightness of  $9280 \text{ L mol}^{-1} \text{ cm}^{-1}$ . The  $\lambda_{\text{abs}}(\text{max})$ ,  $\epsilon_{\text{max}}$ , and  $\Phi_f$  values of the associated phenolate form of C.SNAFL-1 are 540 nm,  $5.2 \times 10^4 \text{ L mol}^{-1} \text{ cm}^{-1}$ , and 0.08,<sup>[2,3,26]</sup> respectively, yielding a lower brightness of  $4160 \text{ L mol}^{-1} \text{ cm}^{-1}$ .

**Fluorescence decay of **I** in organic solvents:** To study the time-resolved fluorescence of **I**, fluorescence decay histograms in different solvents were collected as a function of emission wavelength. In all solvents used, the fluorescence decay profiles could be described by a single-exponential decay function. The lifetimes  $\tau$  estimated by single-curve analysis were independent of the observation wavelength  $\lambda_{\text{em}}$ . Simultaneous (i.e., global) curve fitting of the fluorescence decay surface measured as a function of  $\lambda_{\text{em}}$  with one linked  $\tau$  value confirmed that the decays are indeed mono-exponential and do not depend on the emission wavelength. The results of the time-resolved fluorescence experiments are also listed in Table 1. The  $\tau$  values of **I** are practically solvent independent ( $\tau = 3.9 \pm$

Table 1. Spectroscopic/photophysical data of **I** in different solvents at 20 °C.

Solvent <sup>[a]</sup>	$\lambda_{\text{abs}}(\text{max})$ [nm]	$\epsilon_{\text{max}}^{\text{[b]}}$ [ $\text{L mol}^{-1} \text{ cm}^{-1}$ ]	$\lambda_{\text{em}}(\text{max})$ [nm]	$\text{fwhm}_{\text{abs}}$ [ $\text{cm}^{-1}$ ]	$\Delta\bar{\nu}^{\text{[c]}}$ [ $\text{cm}^{-1}$ ]	$\Phi_f^{\text{[d]}}$	$\tau^{\text{[e]}}$ [ns]	$k_f^{\text{[f]}}$ [ $10^8 \text{ s}^{-1}$ ]	$k_{nr}^{\text{[g]}}$ [ $10^8 \text{ s}^{-1}$ ]
toluene	575		588	790	385	1.00	3.68	2.7	0.00
chloroform	572	$(3.8 \pm 0.3) \times 10^4$	589	859	505	0.93	3.96	2.3	0.18
cyclohexane	573		589	979	474	0.78	3.76	2.1	0.59
tetrahydrofuran	571		588	801	506	0.95	3.77	2.5	0.13
ethyl acetate	568	$(5.0 \pm 0.6) \times 10^4$	585	809	512	0.88	3.86	2.3	0.31
acetonitrile	563		582	824	580	0.88	4.23	2.1	0.28
methanol	562	$(4.2 \pm 0.5) \times 10^4$	577	796	463	0.94	3.84	2.4	0.16

[a] The solvents are ordered according to decreasing polarizability (as measured by the refractive index  $n$ ). [b] Molar absorption coefficients at  $\lambda_{\text{abs}}(\text{max})$ . [c] Stokes shift  $\Delta\bar{\nu} = 1/\lambda_{\text{abs}}(\text{max}) - 1/\lambda_{\text{em}}(\text{max})$ . [d] The standard uncertainties of the fluorescence quantum yields  $\Phi_f$  were determined to be in the range 1–10%. [e] The standard errors on all lifetimes  $\tau$  are  $\leq 10$  ps. [f] Fluorescence deactivation rate constant. [g] Nonradiative deactivation rate constant.

0.2 ns). The values of the fluorescence deactivation rate constant  $k_f$ , calculated according to Equation S15 (Supporting Information) from  $\Phi_f$  and the globally estimated  $\tau$  values, are shown to be independent of the solvent used, with a mean value of  $k_f = (2.4 \pm 0.2) \times 10^8 \text{ s}^{-1}$ . The rate constants of radiationless deactivation  $k_{nr}$ , calculated according to Equation S16 (Supporting Information), are also compiled in Table 1.

**pH dependence of II:** Imidazole in aqueous solution has two pH-dependent acid–base equilibria, characterized by  $pK_a$  values of 7 (protonated–neutral imidazole) and 14 (neutral–anionic imidazole).<sup>[14]</sup> Fluorescent probe **II** with an imidazolyl group will show comparable behavior (Figure 3).

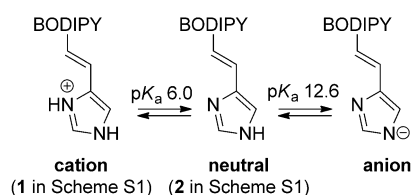


Figure 3. pH-dependent acid–base equilibria of the imidazole group of **II**.

**Visible absorption spectroscopy of II in aqueous (buffer) solution:** Spectrophotometric and fluorometric titrations (vide infra) show that UBimi **II** in aqueous solution has two pH dependent acid–base equilibria, characterized by  $pK_a$  values around 6 (protonated–neutral) and 12.6 (neutral–anionic). At near-neutral pH, only the neutral and cationic forms of **II** are relevant (Figure 3). The visible absorption spectra of aqueous solutions of **II** in the pH range between 5.44 and 8.12 in acetate buffer with different KCl concentrations and in phosphate buffer with different KCl concentrations were recorded. The experimental absorption spectra of **II** at different pH show pH-induced transitions in the pH regions dictated by the ground-state  $pK_a$  value. Figure 4a shows an example of the visible absorption spectra recorded for **II** at different pH values in 50 mM acetate buffer in the absence of KCl. In slightly basic solution, the spectrum is composed of a band characterized by a sharp maximum at 560 nm and a small shoulder around 520 nm. When the pH decreases, the peak at 560 nm is blueshifted to 547 nm, its absorbance decreases, and the shoulder is blueshifted, too. In the pH range 5.44–8.12, two isosbestic points can be clearly distinguished, at 530 and 545 nm. The experimental visible absorption spectra of **II** at pH values ranging between 5.44 and 8.12 show that one pH-induced transition at near-neutral pH is involved. The isosbestic points are consistently positioned at 530 and 545 nm, independent of the acetate or phosphate concentration. Therefore, it is concluded that the acetate or phosphate buffer does not significantly perturb the absorption spectrum of aqueous solutions of **II**, because **II** does not form ground-state complexes with these buffers.

Assuming the acid–base equilibria between the prototropic forms depicted in Figure 3, the apparent acidity constant  $pK_a^{app}$  of the cation–neutral equilibrium can be determined

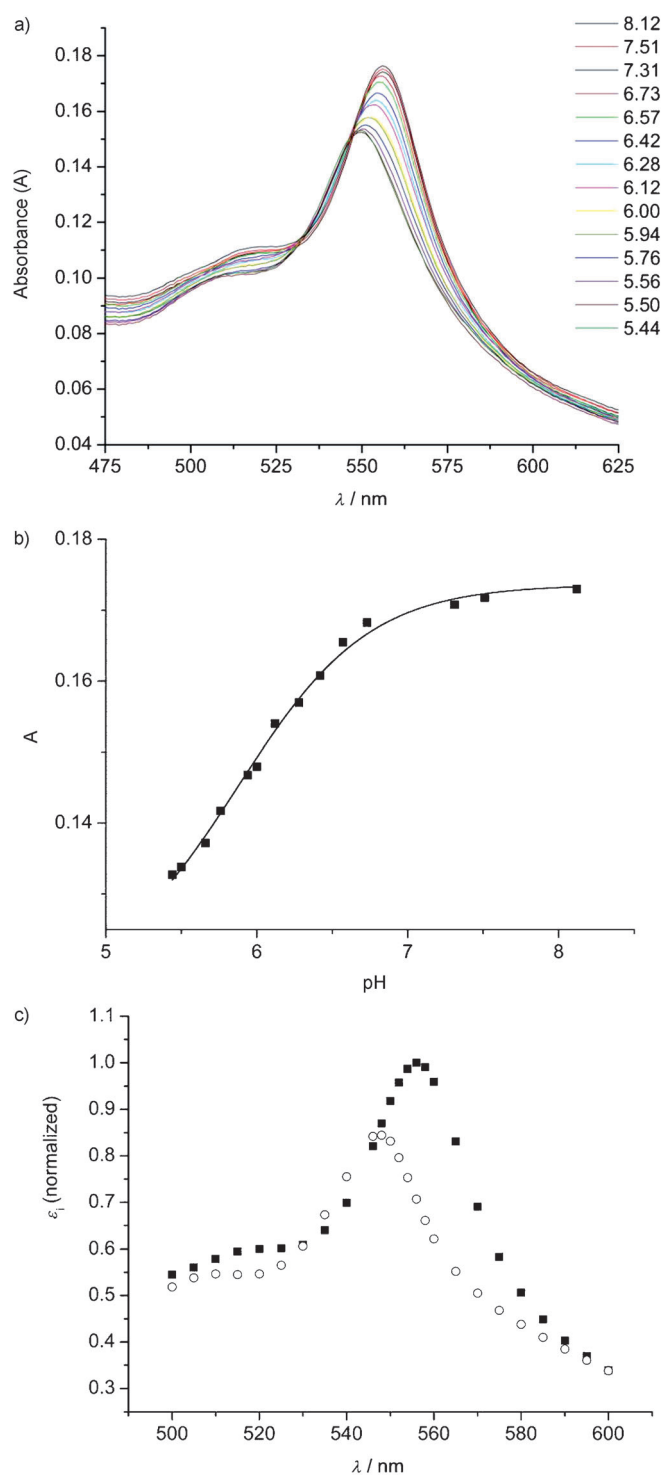


Figure 4. a) Visible absorption spectra of **II** in 50 mM acetate buffer and in the absence of KCl, at pH values between 5.44 and 8.12. b) Global nonlinear least-squares curve fitting of Equation S17 (Supporting Information) to the absorbance  $A_{560}$  at 560 nm versus pH. c) Recovered  $\epsilon_c$  (cationic **1**,  $\circ$ ) and  $\epsilon_n$  (neutral **2**,  $\blacksquare$ ) values of **II** in 50 mM acetate buffer in the presence of 75 mM KCl. The values are normalized to the maximum value of  $\epsilon_n$ .

by using the experimental absorbance changes. A typical data surface of absorbance  $A$  versus pH versus  $\lambda_{abs}$  at each

buffer concentration and ionic strength was composed of 12 pH values and 100  $\lambda_{\text{abs}}$  values between 450 and 650 nm. Beer's law for two prototropic species turned out to be the best model to fit Equation S17 (Supporting Information) to the experimental absorption data. A plot of the absorbance  $A_{560}$  at 560 nm versus pH is shown in Figure 4b. In the data-surface fitting process, the estimated parameters were independent of the initial guesses assigned to these parameters. Figure 4c shows the  $\varepsilon(\lambda)$  values of the cationic ( $\varepsilon_{\text{C}} = \varepsilon_1$ ) and neutral ( $\varepsilon_{\text{N}} = \varepsilon_2$ ) forms of **II**, normalized by the maximum value of  $\varepsilon_{\text{N}}$ , recovered from the fitting of the experimental absorption data of **II** in 50 mM acetate buffer in the presence of 75 mM KCl. These molar absorption coefficient ratios were practically independent of the ionic strength. Since absolute values of  $\varepsilon_{\text{C}}$  and  $\varepsilon_{\text{N}}$  cannot be obtained (see Preparation of **II** in Experimental Section), the brightness of the cationic and neutral forms of **II** cannot be determined. The blueshift of the absorption spectrum of the cationic versus the neutral form of **II** is clearly visible.

**pH dependence of the excitation and emission spectra of **II** in the near-neutral pH region:** Figure 5 displays the fluorescence excitation and emission spectra of UBimi **II** as a function of pH in the pH range 4.5–7.0 in aqueous buffer solution [50 mM 3-(*N*-morpholino)propanesulfonic acid (MOPS)] at room temperature. The excitation spectra (Figure 5a) show a decrease of the excitation band at 556 nm (pH 7.0) and a blueshift to 547 nm (pH 4.5) with increasing  $\text{H}^+$  concentration (lower pH). Thus, the excitation band of the cationic form of **II** is blueshifted by about 10 nm in comparison with that of the neutral form. A pseudo-isoemissive point at about 430 nm can be observed. The acidity constant  $K_{\text{a}}$  of the imidazolium–imidazole equilibrium of **II** (Figure 3) and the stoichiometry of proton binding by neutral imidazole were determined from direct fluorometric titration as a function of pH by fitting Equation S19 (Supporting Information) to the fluorescence excitation data  $F$ . The results obtained at  $\lambda_{\text{ex}} = 556$  nm (corresponding to the excitation wavelength of the maximum intensity of the neutral form) and  $\lambda_{\text{em}} = 590$  nm indicated a 1:1 stoichiometry and yielded a value of  $5.87 \pm 0.03$  for  $\text{p}K_{\text{a}}$  (inset of Figure 5a). Because there is a shift of the excitation spectra, ratiometric excitation measurements can be performed. A  $\text{p}K_{\text{a}}$  value of  $5.83 \pm 0.04$  was estimated by fitting Equation S20 (Supporting Information) to the fluorescence excitation ratios  $R = F(\lambda_{\text{em}}, \lambda_{\text{ex}}^1) / F(\lambda_{\text{em}}, \lambda_{\text{ex}}^2)$  at  $\lambda_{\text{ex}}^1 / \lambda_{\text{ex}}^2 = 547 / 556$  nm and  $\lambda_{\text{em}} = 590$  nm. A similar data analysis of the ratios  $R$ , taking the wavelength of the pseudo-isoemissive point as  $\lambda_{\text{ex}}^2 = 430$  nm with  $\lambda_{\text{ex}}^1 = 556$  nm and  $\lambda_{\text{em}} = 590$  nm, yielded  $\text{p}K_{\text{a}} = 5.72 \pm 0.06$ . Choosing the wavelength of the pseudo-isoemissive point as  $\lambda_{\text{ex}}^2$  leads to a value of 1 for  $\zeta = F_{\text{min}}(\lambda_{\text{em}}, \lambda_{\text{ex}}^2) / F_{\text{max}}(\lambda_{\text{em}}, \lambda_{\text{ex}}^2)$  in Equation S20 (Supporting Information) for the excitation ratiometric method. Nonlinear fits of Equation S20 (Supporting Information) to the ratiometric excitation fluorometric data of **II** in aqueous buffered solution in the presence of KCl are shown in Figure S3 (Supporting Information).

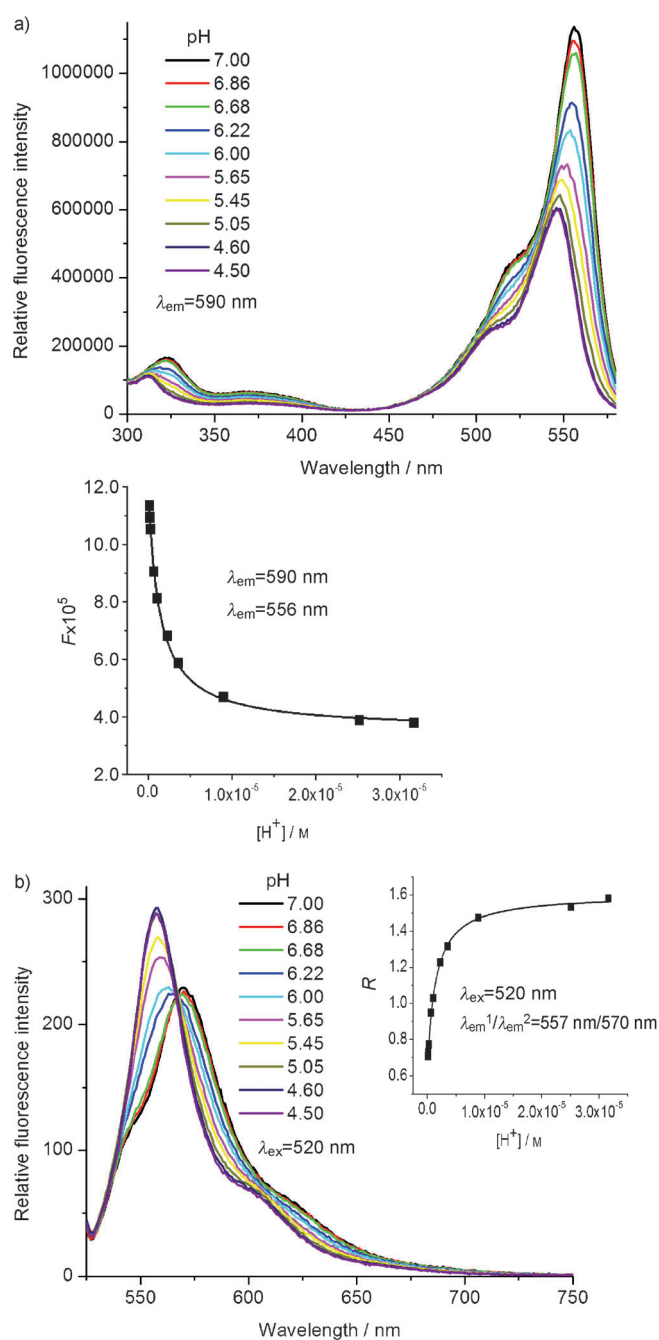


Figure 5. a) Fluorescence excitation spectra (observation wavelength  $\lambda_{\text{em}} = 590$  nm) and b) emission spectra (excitation wavelength  $\lambda_{\text{ex}} = 520$  nm) of **II** in aqueous buffered solution (50 mM MOPS) as a function of pH. The full lines in the insets of a) and b) show the best fits (with  $n = 1$ ) to the direct excitation (a, Equation S19 of the Supporting Information) and ratiometric emission (b, Equation S20 of the Supporting Information) titration data of **II** as a function of  $[\text{H}^+]$ .

The fluorescence emission spectra of **II** as a function of pH (Figure 5b) show a shift of the maximum from 570 nm (pH 7.0) to 557 nm (pH 4.5) with a pseudo-isoemissive point at 567 nm. The fluorescence quantum yield of the neutral (i.e., imidazole) form ( $\Phi_{\text{f}} = 0.8$ ) is higher than that of the cationic (i.e., imidazolium) form ( $\Phi_{\text{f}} = 0.6$ ); pH indicator **II**

emits intense green-yellow fluorescence at lower pH and intense orange fluorescence at higher pH (Figure 6).

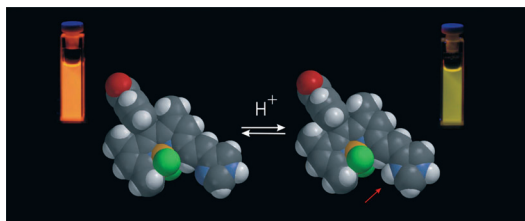


Figure 6. Photograph of the fluorescence emitted by the neutral (orange) and cationic (green-yellow) forms of UBimi **II** due to excitation at 366 nm. The red arrow indicates where protonation takes place.

Direct and ratiometric fluorometric titrations were used to estimate values for the stoichiometry of proton binding and  $K_a$ . For example, direct emission fluorometric titration according to Equation S19 (Supporting Information) at  $\lambda_{\text{ex}} = 520$  nm and  $\lambda_{\text{em}} = 557$  nm gave a  $\text{p}K_a$  of  $6.00 \pm 0.05$ . Conversely, a value of  $5.93 \pm 0.02$  was estimated from ratiometric measurements to be  $\lambda_{\text{em}}^1/\lambda_{\text{em}}^2 = 557/570$  nm, in excellent agreement with previous values. Selecting the wavelength of the pseudo-isoemissive point as  $\lambda_{\text{em}}^2$  gives a value of 1 for  $\xi = F_{\text{min}}(\lambda_{\text{em}}, \lambda_{\text{ex}}^2)/F_{\text{max}}(\lambda_{\text{em}}, \lambda_{\text{ex}}^2)$  in Equation S20 (Supporting Information) for the emission ratiometric method. A mean  $\text{p}K_a$  value of  $5.9 \pm 0.1$  was obtained from all direct and ratiometric fluorometric titrations by using excitation or emission data of **II** in 50 mM MOPS buffered aqueous solution (Table 2). This value matches that obtained by means of absorption measurements in aqueous 50 mM acetate buffer solution (Table 2). These fluorometric and spectrophotometric titration data show that substitution of imidazolium (with  $\text{p}K_a \approx 7.0$ )<sup>[14]</sup> with a difluoroboron dipyrromethene subunit lowers its  $\text{p}K_a$  to about 6.0, that is, BODIPY is indeed electron-withdrawing. Similar effects on the  $\text{p}K_a$  of phenol- and naphthol-substituted BODIPY derivatives have been reported.<sup>[5,10,11]</sup>

**pH dependence of **II** in the alkaline pH region:** Figure S4 (Supporting Information) displays the excitation and emission spectra of **II** as a function of pH (10.75–12.54) in pure water (i.e., without added buffer or salt). The fluorescence excitation spectra of **II** show a decrease of the band with a maximum at 556 nm with increasing pH and a pseudo-isoemissive point at 430 nm. The emission spectra of **II** exhibit two bands with maxima at about 545 and about 570 nm. With increasing  $[\text{H}^+]$  (lower pH), the 545 nm band remains almost constant, while the 570 nm emission band increases in intensity. Values for the acidity constant  $K_a$  of imidazole (neutral form) were determined from direct fluorescence excitation and emission data  $F$  (Equation S19, Supporting Information) and  $R$  values from ratiometric emission data (Equation S20, Supporting Information) at various excitation/emission wavelengths, and yielded a median  $\text{p}K_a$  value of  $12.61 \pm 0.03$  (Table 2). Figure S5 (Supporting Information)

Table 2. Apparent  $\text{p}K_a$  values of UBimi **II** at 20°C determined by absorbance (Equation S17, Supporting Information), and direct (Equation S19, Supporting Information) and ratiometric (Equation S20, Supporting Information) fluorometric titrations in the absence/presence of added buffer and salt (KCl). For the fluorometric titrations, between 5 and 12  $\text{p}K_a$  measurements were included in the calculation of average and standard uncertainty for each experimental condition. The last two entries refer to the neutral–anion equilibrium, and all the other entries to the neutral–cation equilibrium.

Experimental conditions		$\mu$ <sup>[a]</sup>	$\text{p}K_a$ <sup>[b]</sup>	$\text{p}K_a$ <sup>[c]</sup>
Buffer [M]	KCl [M]			
0	0	0	$5.87 \pm 0.07$	$6.03 \pm 0.06$
MOPS (0.01)	0	0.01		$5.91 \pm 0.09$
MOPS (0.05)	0	0.05		$5.88 \pm 0.09$
acetate (0.05)	0	0.05	$5.9 \pm 0.1$	
phosphate (0.05)	0	0.1		$6.2 \pm 0.2$
0	0.1	0.1		$6.0 \pm 0.1$
acetate (0.125)	0	0.125	$5.92 \pm 0.05$	
phosphate (0.075)	0	0.15	$5.89 \pm 0.05$	
phosphate (0.05)	0.1	0.2		$6.01 \pm 0.05$
acetate (0.1)	0.2	0.3	$5.96 \pm 0.06$	
phosphate (0.175)	0	0.35	$5.96 \pm 0.03$	
phosphate (0.175)	0.1	0.45	$5.99 \pm 0.04$	
acetate (0.1)	0.6	0.7	$5.96 \pm 0.08$	
acetate (0.1)	0.9	1.0	$5.98 \pm 0.07$	
0	0	0		$12.61 \pm 0.03$
0	0.1	0.1		$12.63 \pm 0.06$

[a] Ionic strengths  $\mu$  were calculated for solutions at 20°C and pH 6.8 for phosphate buffer, pH 7.2 for MOPS buffer, and 4.76 for acetate buffer (these pH values correspond to the  $\text{p}K_a$  values of the respective buffers, denoted by  $\text{p}K_a^{\text{B}}$ , at 20°C). [b] Determined from spectrophotometric measurements. [c] Determined from fluorometric measurements.

shows an example of nonlinear fit of Equation S20 (Supporting Information) to the ratiometric fluorescence emission data of **II** at alkaline pH (10.75–12.54). Addition of 100 mM KCl gave an almost identical average  $\text{p}K_a$  value of  $12.63 \pm 0.06$ . Our fluorometric titration data indicate that when imidazole (with  $\text{p}K_a \approx 14$  in the alkaline pH range)<sup>[14]</sup> is substituted with BODIPY at the 3-position (as in **II**), its  $\text{p}K_a$  value drops by more than one unit (to 12.6), once more confirming the electron-withdrawing power of BODIPY. An overall view of the pH dependence of  $\Phi_f$  of **II** is shown in Figure S6 (Supporting Information).

**Influence of ionic strength on  $K_a^{\text{app}}$  of **II**:** Since the ionic strength affects the ratio of the concentrations of the cationic and neutral forms, and hence the optical signal from UBimi, a comprehensive study of the dependence of  $K_a^{\text{app}}$  on the ionic strength  $\mu$  is of interest. To study the influence of added buffer and salt on  $K_a^{\text{app}}$  of **II**, we recorded pH-dependent UV/Vis absorption and fluorescence excitation and emission spectra of **II** in aqueous solutions with different concentrations of buffer (MOPS, acetate, and  $\text{H}_2\text{PO}_4^-/\text{HPO}_4^{2-}$ ) and KCl. The steady-state fluorescence spectra were analyzed according to Equations S19 and S20 (Supporting Information) to estimate  $K_a$ . For the global analysis of the absorbance, Equation S17 (Supporting Information) was used. The recovered  $\text{p}K_a^{\text{app}}$  values of **II** at different ionic strengths along with the associated standard uncertainties are listed in Table 2. Increasing ionic strength  $\mu$  only slightly

increases the apparent ground-state acidity constants  $pK_a^{\text{app}}$  up to  $\mu=0.15$ ; thereafter,  $pK_a^{\text{app}}$  is insensitive to ionic strength. Thus, a minor effect of the ionic strength  $\mu$  on the apparent acidity constant of **II** was observed in the  $\mu$  range studied. Moreover, the chemical nature of the buffer is irrelevant. This effect of ionic strength on the apparent acidity constants is in accordance with the Debye–Hückel theory, and is typical of compounds in which the electrolytic charge decreases by the reaction of deprotonation.<sup>[27]</sup> The  $pK_a$  values obtained from fluorometric measurements agree excellently with those from spectrophotometric titrations. The near-independence of  $pK_a^{\text{app}}$  of **II** from ionic strength is a great advantage in fluorescent pH indicators, in which a negligible sensitivity to ionic strength is desired. This negligible sensitivity of **II** to ionic strength is in contrast to some commercially available pH probes, such as BCECF.<sup>[24]</sup>

**Time-resolved fluorescence of II in aqueous solution in the absence/presence of added buffer:** The fluorescence decay traces of **I** in organic solvents were shown to be single-exponential (see above). To test the possibility of applying **II** in fluorescence lifetime imaging (FLIM) in aqueous environment, fluorescence decays were collected first for **II** in pure water followed by decay experiments on addition of buffer. To test the quality of the experimental time-resolved fluorescence data of **II**, each individual fluorescence decay trace measured as a function of emission wavelength  $\lambda_{\text{em}}$ , pH, and analytical buffer concentration  $C^{\text{B}}$  was first analyzed separately by a bi-exponential function in terms of decay times  $\{\tau_1, \tau_2\}$  and associated pre-exponential factors  $\{\alpha_1, \alpha_2\}$ . Such single-curve analysis not only discloses the number of needed exponential terms but also tests the quality of the experimental decay data and allows weeding out of inferior experimental decay data. Traces which gave unacceptable fits as bi-exponentials were eliminated from further analysis.

Secondly, classic global bi-exponential analyses in terms of  $\tau_i$  and  $\alpha_i$  were performed by incorporating in single decay surface curves collected at the same pH and  $C^{\text{B}}$ , but at different  $\lambda_{\text{em}}$ . The decay times  $\tau_i$  were linked (held in common) for decay traces measured at different  $\lambda_{\text{em}}$ . A lot of the bi-exponential fluorescence decays of **II** had an almost negligible contribution corresponding to the shorter decay time  $\tau_2$ . Consequently, in these cases, especially in single-curve analysis, unreliable estimates may be obtained for  $\tau_2$ . It can be expected that the standard global analysis will estimate the  $\{\tau_1, \tau_2\}$  and  $\{\alpha_1, \alpha_2\}$  values with higher accuracy and precision than single-curve analysis. According to the photophysical model presented in Scheme S1 (Supporting Information), the decay times  $\{\tau_1, \tau_2\}$  in the absence of added buffer should be independent of  $\lambda_{\text{em}}$  and pH (within the near-neutral range). Under these circumstances, we have  $\tau_1=(k_{01}+k_{21})^{-1}$  and  $\tau_2=k_{02}^{-1}$ , that is, the photophysical model in the absence of added buffer is not identifiable.<sup>[28]</sup> (For the definition of the rate constants  $k_{ij}$ , see Scheme S1, Supporting Information). Global bi-exponential analysis of the fluorescence decay surface ( $\chi_g^2=1.08$ ) including eleven curves in the absence of buffer (i.e., concentration of buffer  $C^{\text{B}}=0\text{M}$ )

at pH 5.20, 6.82, and 7.45 at  $\lambda_{\text{em}}=560, 570, 580,$  and  $590\text{ nm}$  provided us with reliable decay time estimates:  $\tau_1=4.28\pm 0.04\text{ ns}$  and  $\tau_2=3.3\pm 0.2\text{ ns}$ . Regardless of the initial  $\{\tau_i, \alpha_i\}$  guesses, global curve fitting of these eleven decay curves resulted in the same parameter estimates with the same high precision. The longer lifetimes of **II** are quite close to the values of its corresponding ester form **I** (ca. 4 ns) in various organic solvents (from cyclohexane to acetonitrile). To change the decay times  $\{\tau_1, \tau_2\}$  and to obtain unique estimates for all rate constants defining the photophysical model in Scheme S1 of the Supporting Information (in other words, to have a uniquely identifiable photophysical model), phosphate buffer ( $\text{H}_2\text{PO}_4^-/\text{HPO}_4^{2-}$ ) was added to the aqueous solution of **II**.<sup>[28]</sup> The fluorescence decay times  $\{\tau_1, \tau_2\}$  of **II** at constant pH (6.82) as a function of phosphate buffer concentration  $C^{\text{B}}$  and emission wavelength  $\lambda_{\text{em}}$  were estimated by classical global analysis and are compiled in Table 3. Table 4 lists the globally estimated  $\{\tau_1, \tau_2\}$  of **II** at constant

Table 3. Globally estimated biexponential decay times of **II** in aqueous solution at constant pH (6.82) as a function of total phosphate buffer concentration  $C^{\text{B}}$  and emission wavelength  $\lambda_{\text{em}}$ .

$C^{\text{B}}$ [M]	$\tau_1$ [ns]	$\tau_2$ [ns]	$\chi_g^{2[\text{a}]}$
0	$4.28\pm 0.04$	$3.3\pm 0.2$	1.05
0.05	$4.19\pm 0.04$	$3.3\pm 0.2$	1.04
0.10	$4.06\pm 0.02$	$2.4\pm 0.3$	1.05
0.15	$4.05\pm 0.02$	$2.37\pm 0.09$	1.06
0.25	$4.18\pm 0.02$	$2.23\pm 0.06$	1.10

[a] Equation S21, Supporting Information.

Table 4. Globally estimated bi-exponential decay times of **II** in aqueous solution at constant phosphate buffer concentration  $C^{\text{B}}$  (0.1 M) as a function pH and  $\lambda_{\text{em}}$ .

pH	$\tau_1$ [ns]	$\tau_2$ [ns]	$\chi_g^{2[\text{a}]}$
7.25	$4.03\pm 0.02$	$2.1\pm 0.1$	1.07
7.00	$4.08\pm 0.02$	$2.3\pm 0.1$	1.09
6.82	$4.06\pm 0.02$	$2.5\pm 0.3$	1.05
6.45	$4.12\pm 0.03$	$2.8\pm 0.1$	1.07
6.15	$4.15\pm 0.03$	$2.9\pm 0.2$	1.05
5.80	$4.27\pm 0.03$	$2.9\pm 0.2$	1.10
5.45	$4.28\pm 0.05$	$3.1\pm 0.3$	1.05

[a] Equation S21, Supporting Information.

$C^{\text{B}}$  (0.1 M) as a function of pH and  $\lambda_{\text{em}}$ . In each global bi-exponential analysis reported in Tables 3 and 4, fluorescence decay histograms collected at several  $\lambda_{\text{em}}$  values were combined and analyzed with common (linked)  $\{\tau_1, \tau_2\}$ . Global compartmental analysis of **II** in aqueous solution as a function of pH,  $\lambda_{\text{em}}$ , and pH buffer concentration  $C^{\text{B}}$  was finally used to recover values of all rate constants (Table S1, Supporting Information). The most relevant decay parameters are the deactivation rate constants of the excited cationic ( $k_{01}=2.4\times 10^8\text{ s}^{-1}$ ) and neutral ( $k_{02}=3.0\times 10^8\text{ s}^{-1}$ ) forms of **II**.

**Fluorescence imaging microscopy of UBimi in HEK 293 cells:** Water solubility and membrane permeability are crucial properties for a fluorescent pH indicator that functions

inside live cells. To test whether UBimi fulfills these additional requirements, measurements on live cells were performed. We chose HEK 293 cells because of their large nuclei, which allow one to monitor loading and photobleaching of the probe both in the nuclei and the cytosol. The strategy of delivery of UBimi into cells uses diffusion of the cell membrane permeable ester **I** into cells, where it is hydrolyzed by nonselective intracellular esterases to afford the fluorescent dye **II**.

Based on the fluorescence intensity on excitation at 543 nm of the HEK 293 cells during dye loading (200 nM), it can be concluded that UBimi efficiently accumulates inside the cytosol, but is excluded from the cell nucleus (Figure 7).

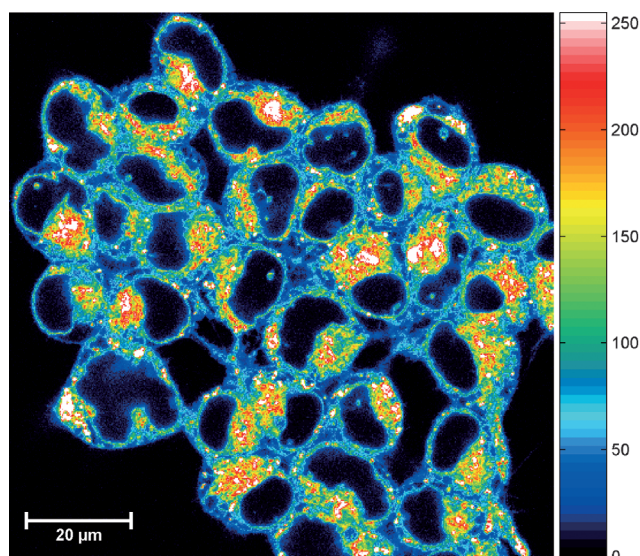


Figure 7. HEK 293 cells stained with UBimi. HEK 293 cells were loaded with 200 nM of Ubimi **I** for 30 min at 21 °C. After rinsing three times with the physiological solution to remove the free probe, the pseudocolor image was collected with a confocal microscope (543 nm excitation, 25.6 μs pixel dwell time, 512 × 512 pixels). The scale of relative intensities is given on the right. UBimi clearly accumulates in the cytosol and not in the cell nucleus, apart from some weak spots possibly indicating nucleoli.

Only small spots in these nuclei, probably nucleoli, display some fluorescence. Bright spots in the cytosol can be noticed and might indicate accumulation in organelles or intracellular vesicles. The efficient accumulation of UBimi also suggests good membrane penetration, which makes the use of pluronic acid obsolete. Images with sufficiently high signal-to-noise ratio can be obtained at other excitation wavelengths (458, 488 nm, 514 nm). Figure S7 (Supporting Information) shows the loading of UBimi in live HEK 293 cells.

The photostability and retention of UBimi in HEK 293 cells were monitored over about 20 min period under a confocal microscope. No significant change in fluorescence signal of UBimi could be observed (Figure S8, Supporting Information). This distinguishes UBimi from most fluorescein-based pH indicators such as BCECF, which bleach relatively quickly.<sup>[29]</sup> Other fluorescein derivatives (e.g., fluorescein diacetate, 6-carboxyfluorescein, and 5,6-dicarboxyfluor-

escein) are not retained well by living cells and rapidly leak out.<sup>[23]</sup>

## Conclusion

Novel BODIPY-derived pH indicator UBimi, available as methyl ester **I** and sodium salt **II**, for the near-neutral pH range with bright fluorescence in the yellow to orange spectral region was synthesized by connecting imidazole to the 3-position of the BODIPY platform through a vinyl bridge. Steady-state and time-resolved fluorescence measurements were employed to study the spectroscopic and photophysical properties of **I** as a function of solvent. The fluorescence lifetime ( $3.9 \pm 0.2$  ns) and fluorescence rate constant ( $k_f = (2.4 \pm 0.2) \times 10^8$  s<sup>-1</sup>) of **I** are independent of the solvent. In aqueous solution, the water-soluble dye **II** undergoes a reversible protonation–deprotonation reaction in the near-neutral pH range that is responsible for the observed spectral shifts of the excitation and emission spectra. The apparent  $pK_a^{app}$  of **II** in aqueous (buffer) solution was obtained by means of absorbance and fluorometric titrations and is practically insensitive to low ionic strength. In aqueous solution in the absence of buffer in the pH range 5.20–7.45, dual-exponential fluorescence decays were obtained with  $\tau_1 = 4.3$  ns for the cationic and  $\tau_2 = 3.3$  ns for the neutral form of **II**. Global compartmental analysis of the fluorescence decay surface of **II** in aqueous solution as a function of  $\lambda_{em}$ , pH, and the absence/presence of phosphate buffer enabled us to estimate all the excited-state rate constants of **II**. The very high  $\Phi_f$  values of the neutral (0.8) and cationic (0.6) forms of **II** in aqueous solution, the possibility of using longer excitation/emission wavelengths, the  $pK_a$  value of 6.0, and the spectral shifts in excitation as well as emission spectra (i.e., dual excitation and dual emission) make this new BODIPY chemosensor an excellent ratiometric fluorescent probe for pH measurements in the pH range 5–7. Dual-emission ratiometric probes allow for fast measurements, because two emission channels can be recorded simultaneously. Methyl ester **I** is readily taken up by biological cells in the cytosol, where it is highly fluorescent and adequately photostable. Recalling the design criteria for the optimal fluorescent pH indicator, one can conclude that building a fluorescent indicator with numerous required properties is feasible, although improvements should be implemented for the construction of a fluorescent indicator useful for intracellular pH sensing and imaging. For cytosolic pH measurements, a better match between the  $pK_a$  of the indicator and physiological pH (6.8–7.4) is desirable. To increase the  $pK_a$  value of the current probe (6.0) one should replace the unsubstituted imidazole group by one with electron-releasing substituents. Although UBimi is retained well inside cells, ideally one may want to increase the number of ester functionalities so that more negatively charged carboxylate groups will be present after their transformation by endogenous esterases. Development of pH chemosensors along these lines is currently in progress.

## Experimental Section

**General aspects:** Details of instrumentation, materials, preparation of solutions, steady-state UV/Vis absorption and fluorescence spectroscopy, time-resolved fluorescence spectroscopy, data analysis of time-resolved fluorescence, cell culture, and fluorescence imaging microscopy are given in the Supporting Information.

Fluorescence decay kinetics and identifiability of a pH probe in the absence/presence of added buffer has been described previously.<sup>[28]</sup> Equations relevant for this study are presented in the Supporting Information.

Details of the determination of  $k_f$  and  $k_{nr}$  from  $\tau$  and  $\Phi_f$ , determination of  $K_a$  and the molar absorption coefficients ratio  $\epsilon_c/\epsilon_n$  from spectrophotometric titration, influence of ionic strength on  $pK_a^{app}$ , and determination of  $K_a$  from direct and ratiometric fluorometric titration are given in the Supporting Information.

**Synthesis of 8-(4-carbomethoxyphenyl)-4,4-difluoro-3-[2-(1H-imidazol-4-yl)ethenyl]-1,5,7-trimethyl-3a,4a-diaza-4-bora-s-indacene (I) (Scheme 1):** 1H-Imidazole-4-carbaldehyde (**IV**, 12 mg, 0.13 mmol) was added to a solution of **III**<sup>[11]</sup> (38 mg, 0.1 mmol) in toluene (5 mL). To this mixture, one drop of piperidine (0.10 mL), one drop of acetic acid (0.10 mL), and a small amount of a molecular sieve were added. The reaction mixture was then heated to reflux for 30 min. After cooling, the crude reaction mixture was purified by silica-gel column chromatography, eluting first with dichloromethane until the starting compound was collected and then changing to 2:1 (v/v) CH<sub>2</sub>Cl<sub>2</sub>/ethyl acetate to afford 21 mg (51 %) of **I** as a violet powder. M.p. the crystal first changes color and does not melt up to 310 °C; <sup>1</sup>H NMR: (300 MHz, CDCl<sub>3</sub>)  $\delta$ =8.21 (d, 2H,  $J$ =8.4 Hz), 7.74 (s, 1H), 7.45 (d, 1H,  $J$ =15.5 Hz), 7.43 (d, 2H,  $J$ =8.2 Hz), 7.32 (s, 1H), 7.28 (d, 1H,  $J$ =16.2 Hz), 6.57 (s, 1H), 6.02 (s, 1H), 3.99 (s, 3H, COOCH<sub>3</sub>), 2.59 (s, 3H), 1.41 (s, 3H), 1.38 ppm (s, 3H); <sup>13</sup>C (75 MHz, CDCl<sub>3</sub>):  $\delta$ =14.5, 14.7, 29.7, 52.3, 116.9, 117.8, 121.5, 128.7, 130.3, 130.9, 136.8, 139.9, 142.4, 153.1, 155.7, 161.9, 166.5 ppm; LRMS (EI, 70 eV):  $m/z$ : 460 [ $M$ ]<sup>+</sup> (100), 440 (90); HRMS (EI, positive):  $m/z$  calcd for C<sub>25</sub>H<sub>23</sub>BF<sub>2</sub>N<sub>4</sub>O<sub>2</sub>: 460.1882 [ $M$ ]<sup>+</sup>, found 460.1876.

**Preparation of II:** To investigate the H<sup>+</sup>-binding properties of the new indicator in aqueous solution, ester **I** was treated with excess base to yield the corresponding water-soluble sodium salt **II**.<sup>[30]</sup> A methanolic solution of **I** was mixed with a highly concentrated solution of 3.5 equiv of spectroscopic-grade NaOH in Milli-Q water. The reaction mixture was heated to reflux for 20 h. The mixture was allowed to cool to RT, more Milli-Q water was added, and the solution was washed with spectroscopic-grade chloroform to extract any residual starting material and possible free-base dipyrromethene side products.<sup>[31]</sup> The separated aqueous layer was evaporated to dryness in a lyophilization apparatus. The lyophilized product was used to prepare solutions of the indicator for further fluorescence measurements. The multistep procedure of converting ester **I** to carboxylate salt **II** (reaction with excess base followed by extraction and finally lyophilization) is not quantitative. Hence, the ultimate amount of **II** in the lyophilized residue is unknown, therefore, it is impossible to obtain absolute values of the absorption coefficients  $\epsilon(\lambda_{ex})$  of **II**, and the brightness of the cationic and neutral forms of **II** cannot be determined. Comparison of the absorption and fluorescence emission spectra of ester **I** in methanol and sodium salt **II** in water indicates that the fluorophore structure remains intact.

## Acknowledgements

The K.U. Leuven authors are grateful to the University Research Fund of the K.U. Leuven for grant IDO/00/001 and for postdoctoral fellowships to W.Q. and M.B. The authors from the K.U. Leuven and the University of Wrocław thank the Flemish Ministry of Science and Technology for a postdoctoral fellowship to A.F. through the Bilateral Scientific and Technological Cooperation Program (grant no. BIL05/16). Dr. A. Stefan is acknowledged for technical help with the single-photon timing experiments. W.Q. thanks the Scientific Research Fund for Introducing

Talented Persons to Lanzhou University. W.Q. is supported by the Program for New Century Excellent Talents in University (NCET-09-0444) and the Fundamental Research Funds for the Central Universities (lzujbky-2011-22). This study was supported in part by the Key Program of National Natural Science Foundation of China (20931003). N.S. is supported by a grant from the Instituut voor de aanmoediging van innovatie door Wetenschap en Technologie in Vlaanderen (IWT). M.A. acknowledges support from tUL-impuls. This work was supported in part by grant P07-FQM-3091 from the Consejería de Innovación, Ciencia y Empresa (Junta de Andalucía).

- [1] a) *Chemosensors of Ion and Molecule Recognition* (Eds.: J.-P. Desvergne, A. W. Czarnik), Kluwer, Dordrecht, The Netherlands, **1997**; b) B. Valeur, *Molecular Fluorescence. Principles and Applications*, Wiley-VCH, Weinheim, Germany, **2002**.
- [2] R. P. Haugland, *The Handbook. A Guide to Fluorescent Probes and Labeling Technologies*, 10th ed., Molecular Probes, Eugene, Oregon, **2005**, pp. 935–955.
- [3] J. Han, K. Burgess, *Chem. Rev.* **2010**, *110*, 2709–2728.
- [4] A. Treibs, F.-H. Kreuzer, *Justus Liebigs Ann. Chem.* **1968**, *718*, 208–223.
- [5] a) A. Loudet, K. Burgess, *Chem. Rev.* **2007**, *107*, 4891–4932; b) G. Ulrich, R. Ziessel, A. Harriman, *Angew. Chem.* **2008**, *120*, 1202–1219; *Angew. Chem. Int. Ed.* **2008**, *47*, 1184–1201.
- [6] T. Gareis, C. Huber, O. S. Wolfbeis, J. Daub, *Chem. Commun.* **1997**, 1717–1718.
- [7] C. N. Baki, E. U. Akkaya, *J. Org. Chem.* **2001**, *66*, 1512–1513.
- [8] M. Kollmannsberger, T. Gareis, S. Heintl, J. Breu, J. Daub, *Angew. Chem.* **1997**, *109*, 1391; *Angew. Chem. Int. Ed. Engl.* **1997**, *36*, 1333–1335.
- [9] T. Werner, C. Huber, S. Heintl, M. Kollmannsberger, J. Daub, O. S. Wolfbeis, *Fresenius J. Anal. Chem.* **1997**, *359*, 150–154.
- [10] a) M. Baruah, W. Qin, N. Basarić, W. M. De Borggraeve, N. Boens, *J. Org. Chem.* **2005**, *70*, 4152–4157; b) W. Qin, M. Baruah, A. Stefan, M. Van der Auweraer, N. Boens, *ChemPhysChem* **2005**, *6*, 2343–2351.
- [11] W. Qin, M. Baruah, W. M. De Borggraeve, N. Boens, *J. Photochem. Photobiol. A* **2006**, *183*, 190–197.
- [12] Y. Urano, D. Asanuma, Y. Hama, Y. Koyama, T. Barrett, M. Kamiya, T. Nagano, T. Watanabe, A. Hasegawa, P. L. Choyke, H. Kobayashi, *Nature Medicine* **2009**, *15*, 104–109.
- [13] S. E. Braslavsky, *Pure Appl. Chem.* **2007**, *79*, 293–465.
- [14] a) D. D. Perin, *Dissociation Constants of Organic Bases in Aqueous Solutions*, Butterworth, London, **1972**; b) E. P. Serjenge, B. Dempsey, *Ionization Constants of Organic Acids in Aqueous Solution*, Pergamon Press, New York, **1979**; c) N. Isaacs, *Physical Organic Chemistry*, 2nd ed., Longman Scientific & Technical, Harlow, England, **1995**.
- [15] a) K. Rurack, M. Kollmannsberger, J. Daub, *Angew. Chem.* **2001**, *113*, 396–399; *Angew. Chem. Int. Ed.* **2001**, *40*, 385–387; b) K. Rurack, M. Kollmannsberger, J. Daub, *New J. Chem.* **2001**, *25*, 289–292; c) A. Coskun, E. U. Akkaya, *J. Am. Chem. Soc.* **2005**, *127*, 10464–10465; d) M. Baruah, W. Qin, C. Flors, J. Hofkens, R. A. L. Vallée, D. Beljonne, M. Van der Auweraer, W. M. De Borggraeve, N. Boens, *J. Chem. Phys. A* **2006**, *110*, 5998–6009; e) T. Rohand, W. Qin, N. Boens, W. Dehaen, *Eur. J. Org. Chem.* **2006**, 4658–4663; f) W. Qin, T. Rohand, W. Dehaen, J. N. Clifford, K. Driessen, D. Beljonne, B. Van Averbeke, M. Van der Auweraer, N. Boens, *J. Chem. Phys. A* **2007**, *111*, 8588–8597; g) W. Qin, M. Baruah, M. Sliwa, M. Van der Auweraer, W. M. De Borggraeve, D. Beljonne, B. Van Averbeke, N. Boens, *J. Chem. Phys. A* **2008**, *112*, 6104–6114.
- [16] A nonexhaustive list of BODIPY papers with spectroscopic/photophysical data: a) E. Vos de Wael, J. A. Pardo, J. A. van Koeveeringe, J. Lugtenburg, *Recl. Trav. Chim. Pays-Bas* **1977**, *96*, 306–309; b) T. López Arbeloa, F. López Arbeloa, I. López Arbeloa, I. García-Moreno, A. Costela, R. Sastre, F. Amat-Guerri, *Chem. Phys. Lett.* **1999**, *299*, 315–321; c) A. Costela, I. García-Moreno, C. Gomez, R. Sastre, F. Amat-Guerri, M. Liras, F. López Arbeloa, J. Bañuelos

- Prieto, I. López Arbeloa, *J. Phys. Chem. A* **2002**, *106*, 7736–7742; d) F. López Arbeloa, J. Bañuelos Prieto, V. Martínez Martínez, T. Arbeloa López, I. López Arbeloa, *ChemPhysChem* **2004**, *5*, 1762–1771; e) J. Bañuelos Prieto, F. López Arbeloa, V. Martínez Martínez, T. Arbeloa López, F. Amat-Guerri, M. Liras, I. López Arbeloa, *Chem. Phys. Lett.* **2004**, *385*, 29–35; f) W. Qin, M. Baruah, M. Van der Auweraer, F. C. De Schryver, N. Boens, *J. Phys. Chem. A* **2005**, *109*, 7371–7384; g) Z. Dost, S. Atilgan, E. U. Akkaya, *Tetrahedron* **2006**, *62*, 8484–8488; h) W. Qin, T. Rohand, M. Baruah, A. Stefan, M. Van der Auweraer, W. Dehaen, N. Boens, *Chem. Phys. Lett.* **2006**, *420*, 562–568; i) Z. Li, R. Bittman, *J. Org. Chem.* **2007**, *72*, 8376–8382; j) Z. Ekmekci, M. D. Yilmaz, E. U. Akkaya, *Org. Lett.* **2008**, *10*, 461–464; k) L. Li, J. Han, B. Nguyen, K. Burgess, *J. Org. Chem.* **2008**, *73*, 1963–1970.
- [17] H. C. Kang, R. P. Haugland (Molecular Probes, Inc., Eugene, Oregon, USA), US 5187288, **1993**.
- [18] M. Kollmannsberger, K. Rurack, U. Resch-Genger, J. Daub, *J. Phys. Chem. A* **1998**, *102*, 10211–10220.
- [19] a) A. Burghart, H. Kim, M. B. Welch, L. H. Thoresen, J. Reibenspies, K. Burgess, *J. Org. Chem.* **1999**, *64*, 7813–7819; b) H. L. Kee, C. Kirmaier, L. Yu, P. Thamyongkit, W. J. Youngblood, M. E. Calder, L. Ramos, B. C. Noll, D. F. Bocian, W. R. Scheidt, R. R. Birge, J. S. Lindsey, D. Holten, *J. Phys. Chem. B* **2005**, *109*, 20433–20443; c) W. Qin, V. Leen, T. Rohand, W. Dehaen, P. Dedecker, M. Van der Auweraer, K. Robeyns, L. Van Meerelt, D. Beljonne, B. Van Averbeke, J. N. Clifford, K. Driessen, K. Binnemans, N. Boens, *J. Chem. Phys. A* **2009**, *113*, 439–447; d) S. Rihn, P. Retailleau, N. Bugsaliewicz, A. De Nicola, R. Ziessel, *Tetrahedron Lett.* **2009**, *50*, 7008–7013.
- [20] A. Filarowski, M. Kluba, K. Ciešlik-Boczula, A. Koll, A. Kochel, L. Pandey, W. M. De Borggraeve, M. Van der Auweraer, J. Catalán, N. Boens, *Photochem. Photobiol. Sci.* **2010**, *9*, 996–1008.
- [21] E. Lippert, *Z. Naturforsch. A* **1955**, *10*, 541–545.
- [22] N. Mataga, Y. Kaifu, M. Koizumi, *Bull. Chem. Soc. Jpn.* **1955**, *28*, 690–691 and **1956**, *29*, 465–470.
- [23] T. J. Rink, R. Y. Tsien, T. Pozzan, *J. Cell Biol.* **1982**, *95*, 189–196.
- [24] N. Boens, W. Qin, N. Basarić, A. Orte, E. M. Talavera, J. M. Alvarez-Pez, *J. Phys. Chem. A* **2006**, *110*, 9334–9343.
- [25] J. Liu, Z. Diwu, D. H. Klaubert, *Bioorg. Med. Chem. Lett.* **1997**, *7*, 3069–3072.
- [26] J. E. Whitaker, R. P. Haugland, F. G. Prendergast, *Anal. Biochem.* **1991**, *194*, 330–344.
- [27] a) T. Vilariño, S. Fiol, X. L. Armesto, I. Brandariz, M. E. Sastre de Vicente, *J. Chem. Soc. Faraday Trans.* **1997**, *93*, 413–417; b) L. Crovetto, J. M. Paredes, R. Rios, E. M. Talavera, J. M. Alvarez-Pez, *J. Phys. Chem. A* **2007**, *111*, 13311–13320.
- [28] N. Boens, N. Basarić, E. Novikov, L. Crovetto, A. Orte, E. M. Talavera, J. M. Alvarez-Pez, *J. Phys. Chem. A* **2004**, *108*, 8180–8189.
- [29] I. D. Weiner, L. L. Hamm, *Am. J. Physiol. Renal Physiol.* **1989**, *256*, F957–F964.
- [30] N. Basarić, M. Baruah, W. Qin, B. Metten, M. Smet, W. Dehaen, N. Boens, *Org. Biomol. Chem.* **2005**, *3*, 2755–2761.
- [31] S. M. Crawford, A. Thompson, *Org. Lett.* **2010**, *12*, 1424–1427.

Received: August 9, 2010

Revised: April 27, 2011

Published online: August 17, 2011